

Effect of Trace Amounts of Water on Organic Solvent Transport through γ -Alumina Membranes with Varying Pore Sizes

Sankhanilay Roy Chowdhury, Klaas Keizer, Johan E. ten Elshof,* and Dave H. A. Blank

Inorganic Materials Science, MESA⁺ Institute for Nanotechnology & Faculty of Science and Technology, University of Twente, P.O. Box 217, 7500 AE Enschede, The Netherlands

Received December 20, 2003. In Final Form: March 17, 2004

The transport behavior of toluene and *n*-hexane in γ -alumina membranes with different pore diameters was studied. It was shown that the permeability of water-lean hexane and toluene is in agreement with Darcy's law down to membrane pore diameters of 3.5 nm. The presence of molar water fractions of $5\text{--}8\cdot 10^{-4}$ in these solvents led to a permeability decrease of the γ -alumina layer by a factor of 2–4 depending on pore size. In general, a lower permeability was found for hexane than for toluene. Moreover, in the presence of water a minimum applied pressure of 0.5–1.5 bar was required to induce net liquid flow through the membrane. These phenomena were interpreted in terms of capillary condensation of water in membrane pores with a size below a certain critical diameter. This is thought to lead to substantial blocking of these pores for transport, so that the effective tortuosity of the membrane for transport of hydrophobic solvents increases.

1. Introduction

Nanofiltration (NF) membranes are used to separate solvents from multivalent ions and small organic molecules using pressure as driving force. Two parameters are of crucial importance in membrane separation processes, namely, the level of molecule or ion retention and the solvent permeability. The permeability of liquids depends to a large extent on the interactions between solvent and membrane pore surface. This will be a dominant factor especially when narrow pores of a few molecular diameters wide are considered. It has been demonstrated for polymeric membrane how solvent/membrane interactions influence solvent transport.^{1–4} The permeation of pure alcohols as nonaqueous solvents through inorganic membranes has also been discussed in detail.⁵ However, to date only few papers^{6–9} have reported on the application of inorganic nanofiltration membranes to separations of nonaqueous solutions.¹⁰

In this article, we report on the effect of systematic variation of the γ -alumina membrane pore size on the liquid permeation behavior of toluene and *n*-hexane. We demonstrate how the presence of low concentrations of

water affects the liquid permeability of these hydrocarbons considerably. We propose a hypothesis to explain the permeability change of hydrocarbon liquids through γ -alumina membranes in the presence of small amounts of water in the hydrocarbon liquid feed. These phenomena are also of practical importance for industrial liquid separation processes involving mesoporous membranes, since industrial organic solvents usually contain small amounts of water that are not considered explicitly.

2. Experimental Section

2.1. Preparation of α -Alumina Supported Mesoporous γ -Alumina Membranes. The γ -alumina membrane consisted of a macroporous α -alumina support and a thin mesoporous γ -alumina layer. The α -alumina supports were made by colloidal filtration of well-dispersed 0.4 μm α -alumina particles (AKP-30, Sumitomo). The dispersion was stabilized by peptizing with nitric acid. After drying at room temperature, the filter compact was sintered at 1100 °C. Flat disks of \varnothing 39 mm and 2.0 mm thickness were obtained after machining and polishing. The final porosity of these supports is \sim 30% and the average pore diameter is in the range of 80–120 nm. Three different mesoporous γ -alumina membranes of \sim 3- μm thickness were prepared by dip-coating twice the above-mentioned porous α -alumina supports in a boehmite sol, followed by drying and calcining at 450, 600, or 800 °C for 1 h (heating/cooling rates 0.5 °C/min), respectively. These membranes are designated hereafter as γ -450, γ -600, and γ -800, respectively.

2.2. Preparation of γ -Alumina Powder. Three different γ -alumina powders were prepared by drying the boehmite sol in air, followed by calcination at 450, 600, or 800 °C for 1 h (heating/cooling rates 0.5 °C/min), respectively. These powders were subjected to nitrogen adsorption/desorption experiments (Micromeritics) at 77 K.

2.3. Solvent Permeation Experiments. Steady-state liquid flux measurements were carried out in a dead-end nanofiltration cell at room temperature on α -alumina supported γ -alumina composite membranes using water-rich toluene (0.005 mol H₂O/l), water-rich hexane (0.006 mol H₂O/l), water-lean toluene ($<$ 0.001 mol H₂O/l) (Aldrich), and water-lean hexane ($<$ 0.001 mol H₂O/l) (Aldrich). The water concentrations were determined using a Metrohm KFT 756 Karl Fischer coulometer. The volume of the permeation cell is 1000 mL and the operating pressure

* Corresponding author. E-mail: j.e.tenelshof@utwente.nl; phone: +31-53-489-2695; fax: +31-53-489-4683.

(1) Machado, D. R.; Hasson, D.; Semiat, R. *J. Membr. Sci.* **1999**, *163*, 93.

(2) Yang, X. J.; Livingston, A. J.; Freitas dos Santos, L. *J. Membr. Sci.* **2001**, *190*, 45.

(3) Machado, D. R.; Hasson, D.; Semiat, R. *J. Membr. Sci.* **2000**, *166*, 63.

(4) Banushali, D.; Kloos, S.; Kurth, C.; Bhattacharyya, D. *J. Membr. Sci.* **2001**, *189*, 1.

(5) Tsuru, T.; Sudou, T.; Kawahara, S.; Yoshioka, T.; Asaeda, M. *J. Colloid Interface Sci.* **2000**, *228*, 292.

(6) Roy Chowdhury, S.; Schmuhl, R.; Keizer, K.; ten Elshof, J. E.; Blank, D. H. A. *J. Membr. Sci.* **2003**, *225*, 177.

(7) Knudstrup, T. G.; Bitsanis, I. A.; Westermannclark, G. B. *Langmuir* **1995**, *11*, 893.

(8) Font, J.; Castro, R. P.; Cohen, Y. *J. Colloid Interface Sci.* **1996**, *181*, 347.

(9) Tsuru, T.; Miyawaki, M.; Kondo, H.; Yoshioka, T.; Asaeda, M. *Sep. Purif. Technol.* **2003**, *32*, 105.

(10) Sarrade, S.; Rios, G. M.; Carles, M. *J. Membr. Sci.* **1996**, *114*, 81.

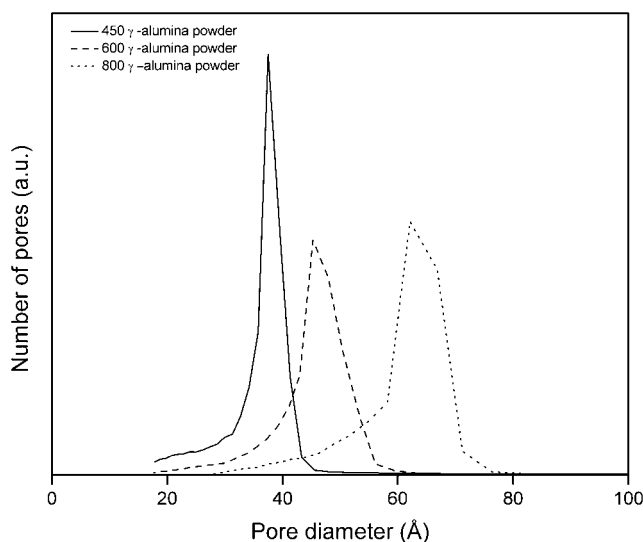


Figure 1. Pore size distribution of γ -alumina powders calcined at 450, 600, and 800 °C.

Table 1. Physical Properties of γ -Alumina Powders

calcination temperature (°C)	BET area (m ² /g)	pore diameter (nm)	porosity (%)
450	373	3.5	55
600	285	4.4	55
800	196	5.9	55

range was kept in the range 2–14 bar. The stirring speed in the cell was kept constant at 200 rpm throughout all experiments. Liquid permeation experiments were done on fresh membranes for each run. Liquid permeation tests with water-lean solvents were carried out in the presence of 1-nm pore-sized dry molecular sieves (2-mm bead diameter, Merck) inside the permeation vessel to remove trace amounts of moisture from the vessel. Fluxes were measured with increasing and decreasing pressure steps after reaching (pseudo-)steady state conditions, and all measurements were usually done within the first 3 h of operation of the membrane. Permeation tests with water-rich and water-lean hexane for longer times to observe the effect of operation time on membrane permeability were carried out on γ -450 membranes at a constant pressure of 8.6 bar.

3. Results

The γ -450, γ -600, and γ -800 powders were subjected to nitrogen adsorption/desorption experiments. From Figure 1, it can be seen that the pore size increases and the pore size distribution becomes broader with increasing calcination temperature. The main physical properties of the powders are listed in Table 1.

Figure 2 shows the volumetric solvent fluxes versus applied pressure through γ -800 membranes with water-rich hydrocarbons. According to Darcy's law, when the transport mechanism obeys the viscous flow model, the flux is proportional to the applied pressure, irrespective of the type of liquid. The mathematical formulation of Darcy's law is¹¹

$$J = -\frac{1}{\eta} k_p \Delta P \quad (1)$$

where J is the volumetric flux, η the bulk liquid viscosity, and ΔP the applied pressure difference across the membrane. The membrane permeability coefficient k_p of a single

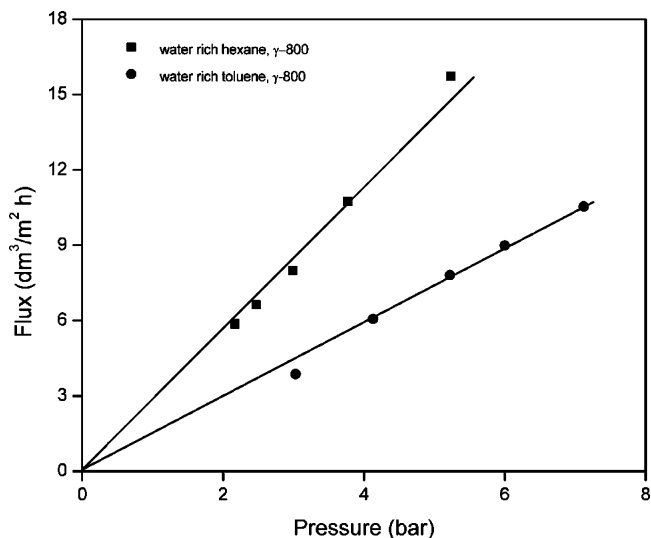


Figure 2. Volumetric liquid fluxes versus applied pressure through γ -800 membranes.

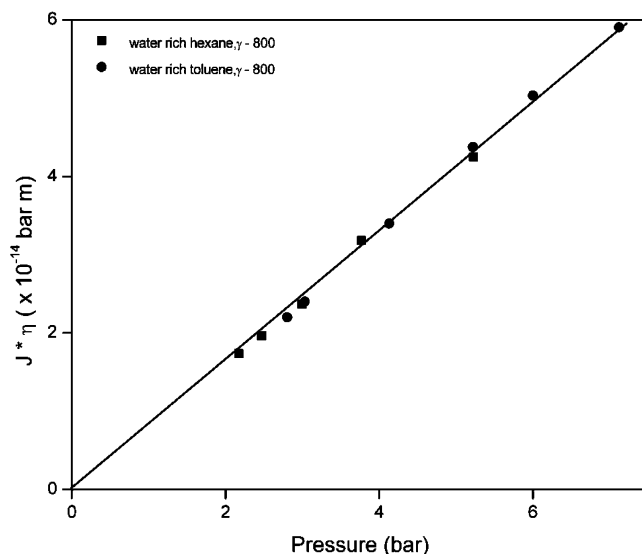


Figure 3. Product of volumetric liquid flux and liquid viscosity versus applied pressure through γ -800 membranes.

membrane layer with pore radius r is defined as¹²

$$k_p = \frac{\epsilon r^2}{8\tau L} \quad (2)$$

where ϵ is the porosity of the membrane material, τ the tortuosity of the membrane layer, and L the membrane layer thickness. From eq 2 it is clear that k_p is a constant that depends only on the structural properties of the membrane material, not on the physical properties of the permeating liquid. This is illustrated in Figure 3, which shows the product of flux and solvent viscosity as a function of applied pressure. The slope of the fitted straight line is the overall permeability coefficient k_m of the membrane for a given solvent. It is clear that the permeability through γ -800 membranes with a pore diameter of 6–8 nm is not influenced by the nature of the solvent.

Figure 4 shows similar viscosity-corrected fluxes of water-rich hydrocarbons through γ -600 and γ -450 membranes. In comparison with Figure 3, some remarkable features are observed. Both toluene and hexane require

(11) Gieselmann, M. J. *Langmuir* **1992**, *8*, 1342.

(12) Mulder, M. *Basic principles of membrane technology*; Kluwer Academic Press: Dordrecht, The Netherlands, 1996; Chapter 5.

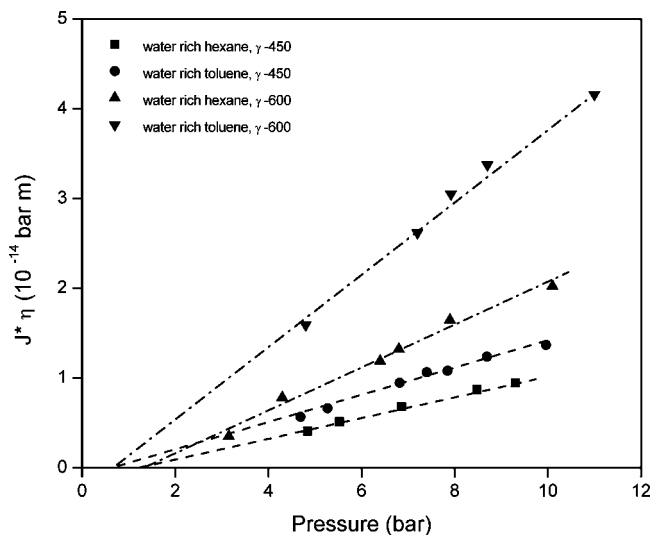


Figure 4. Product of volumetric liquid flux and liquid viscosity versus applied pressure through γ -600 and γ -450 membranes.

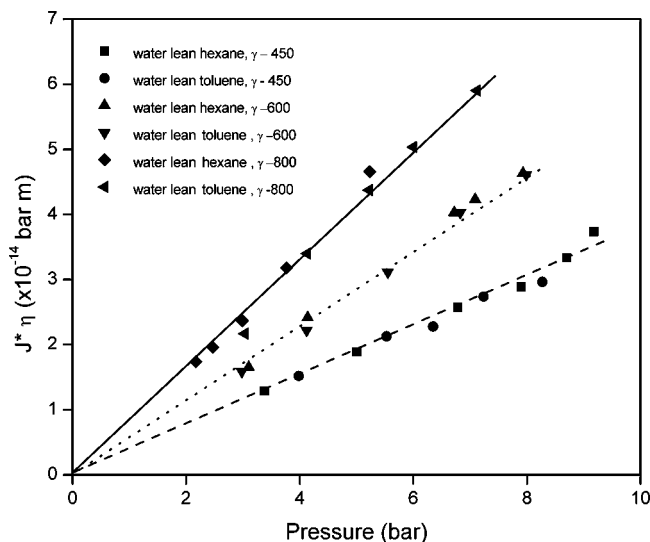


Figure 5. Product of volumetric liquid flux and liquid viscosity versus applied pressure of water-lean solvents.

a certain threshold pressure to be exceeded before transport through the γ -alumina membranes is observed. These two liquids also have different permeability coefficients, and it appears that the permeability of hexane through γ -alumina is smaller than that of toluene.

Figure 5 shows viscosity-corrected fluxes of water-lean liquids through γ -800, γ -600, and γ -450 membranes. Comparison with the data in Figures 3 and 4 shows that the permeabilities of these liquids through γ -450 and γ -600 are 2–4 times higher than the permeabilities of the corresponding water-rich liquids through the same membranes. Moreover, in contrast to water-rich liquids, no threshold pressure for liquid transport with water-lean liquids was observed within experimental error.

Figure 6 shows the time dependence of water-lean and water-rich hexane fluxes at constant pressure through γ -450 membranes. The figure shows that both liquid fluxes decrease with time, but the permeability decrease of water-rich hexane occurs slightly faster.

4. Discussion

The experiments showed that when water-lean or water-rich hexane or toluene pass through membranes with relatively large pores, for example, the γ -800 membrane

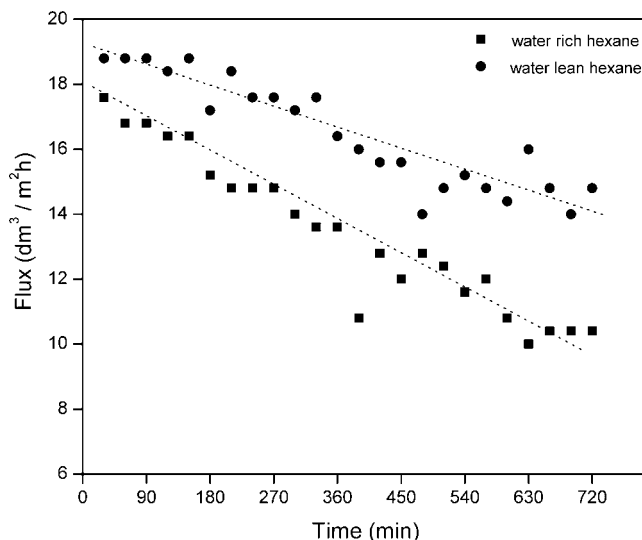


Figure 6. Volumetric fluxes of water-lean and water-rich hexane through a γ -450 membrane at constant applied pressure of 8.6 bar. Drawn lines serve as guide to the eye.

Table 2. Permeability Coefficients k_γ of Water-Lean and Water-Rich Organic Liquids through Mesoporous γ -Alumina Membrane, Calculated from Eq 3

solvent	permeability coefficient k_γ (10^{-14} m)		
	γ -800	γ -600	γ -450
water-rich hexane	3.1 ± 0.22	0.30 ± 0.063	0.13 ± 0.011
water-rich toluene	3.1 ± 0.26	0.66 ± 0.13	0.19 ± 0.034
water-lean hexane	3.1 ± 0.29	1.32 ± 0.15	0.54 ± 0.059
water-lean toluene	3.1 ± 0.15	1.32 ± 0.085	0.54 ± 0.044

Table 3. Tortuosities of Mesoporous Top Layers Calculated from Eq 2

mesoporous top layer	tortuosity τ
γ -800	6.4 ± 1.2
γ -600	8.2 ± 1.6
γ -450	16 ± 1.8

with ~ 6 nm pores, the permeability coefficients of all liquids are the same, and the liquid behavior appears to obey Darcy's law, eq 1.

The overall transport resistance of liquids through a stacked α -alumina/ γ -alumina membrane can be regarded as a series of two transport resistances in series. The overall membrane permeability coefficient k_m can therefore be deconvoluted into the permeabilities of the individual layers according to⁶

$$1/k_m = 1/k_\alpha + 1/k_\gamma \quad (3)$$

where k_α and k_γ are the permeability coefficients of the α -alumina support ($k_\alpha = 1.17 \cdot 10^{-14}$ m) and the mesoporous γ -alumina top layer, respectively. Table 2 summarizes the k_γ values of different γ -alumina top layers for different liquids. The permeabilities of water-lean toluene and hexane in all three membranes appear to follow Darcy's law, that is, these k_γ values and the values of pore size and porosity as presented in Table 1; the effective τ values of the mesoporous top layers were calculated from eq 2. Table 3 lists these τ values. The tortuosities of the γ -800 and γ -600 membranes fall in the range of tortuosities of 5–13 reported in the literature for γ -800,¹³ while a slightly larger τ value is found for γ -450. It is known that the crystallite shape of the primary oxide particles is one of

(13) Leenaars, A. F. M.; Burggraaf, A. J. *J. Membr. Sci.* **1985**, *24*, 245.

Table 4. Threshold Pressure for Water-Rich Solvent Transport through Mesoporous Alumina Membrane

solvent	threshold pressure (bar)	
	γ -600	γ -450
water-rich hexane	0.86 \pm 0.34	1.36 \pm 0.20
water-rich toluene	0.85 \pm 0.37	1.34 \pm 0.28

the main parameters that controls the tortuosity τ of a porous material.¹³ For spherical particles τ has a value close to 5, but for platelet-shaped crystallites its value will be larger. Since the morphology of γ -alumina crystallites changes from plateletlike into spherical with increasing calcination temperature,¹³ the τ -values listed in Table 3 reflect the change of crystallite shape with increasing calcination temperature.¹³

According to the data in Figure 4 and Table 2, the permeability coefficients appear to depend on the nature of the permeating liquid when the pore size is smaller than in γ -800 and water-rich hydrocarbons are employed. Moreover, the permeabilities of the water-rich hydrocarbons are substantially smaller than those of the corresponding water-lean equivalents, while the transport of water-rich liquids through γ -600 and γ -450 also requires a nonzero threshold pressure to be exceeded before net transport occurs. These phenomena are in disagreement with Darcy's law. The threshold pressures of the different liquids through γ -450 and γ -600 membranes, calculated from the intercepts of the extrapolated flux versus pressure plots, are listed in Table 4.

Several factors may possibly contribute to these effects and they should be considered in order to interpret the permeability differences between different solvent-membrane combinations. The first factor to consider is the extent to which the use of bulk liquid viscosities in eq 1 is still allowed. It has been reported that the density and viscosity of non-hydrogen-bonded liquids that are confined between two smooth surfaces can be strongly influenced by the close presence of these surfaces.^{14,15} However, the roughness of the internal γ -alumina membrane surfaces that are considered in the present study will probably smear out the solvation forces¹⁶ that are responsible for the density gradient in a liquid in narrow confinement.¹⁴ This suggests that mostly van der Waals type of interactions occurs between liquid molecules and pore wall and that the liquid viscosities in these 4–7-nm wide pores will therefore be similar to the viscosities of the corresponding bulk liquids.

The second factor is the possibility of phase separation of water from hydrocarbon-water binary liquids. This process can be regarded as a conventional capillary condensation process occurring in systems of poorly miscible liquids and was described experimentally by Christenson^{16–19} and theoretically by Evans.²⁰ A phase-separated water phase may form capillary water bridges in narrow pores, effectively leading to complete blocking of these pores for transport.¹⁷ In thermodynamic equilibrium phase separation and subsequent capillary condensation of the water phase in a pore with an effective Kelvin radius, r_K will occur spontaneously when

$$r_K < \frac{-\gamma_{sw} V_m}{RT \ln(x_w \chi_w)} \quad (4)$$

where x_w and χ_w are the molar fraction of water and the

activity coefficient of water in the solvent, respectively, γ_{sw} is the surface tension between water and hydrocarbon, V_m is the molar volume of water, and R and T are the gas constant and temperature, respectively. The surface tensions γ_{sw} of water-hexane and water-toluene can be estimated to be ~ 50 mN/m.²¹ For very dilute solutions, the product $x_w \chi_w$ can be replaced by the ratio of water concentration c_w and saturation concentration c_w^0 .²⁰ Since the solubility limit of water in toluene and hexane are ~ 0.015 mol/l and ~ 0.0067 mol/l,²² respectively, the relative activities $x_w \chi_w$ of water in toluene and in hexane are ~ 0.35 and ~ 0.9 , respectively. Hence, the critical pore sizes at which capillary condensation will occur in thermodynamic equilibrium fall in the 1–10 nm range, and the critical pore size is substantially larger for hexane than for toluene. The critical pore size may be different from the predictions of eq 4 under nonequilibrium transport conditions.

Pores that are wider than the critical size predicted by eq 4 will not become completely filled with water, but their effective pore radius (for hydrocarbon transport) may be reduced because of the formation of an annulus water phase that is adsorbed on the pore walls. This phenomenon is more or less similar to the well-known t-layer adsorption of condensable gases on surfaces.²³ In the present case, the formation of a water film will be driven by hydrogen-bonding-type interactions between water and the OH-functional γ -alumina pore walls, which are energetically more favorable than the van der Waals type interactions between hydrocarbon and pore wall.

The physical significance of water bridge formation on hydrocarbon liquid transport is that it decreases the effective porosity ϵ of the membrane medium. More importantly, it also increases the effective tortuosity τ of the membrane medium, because several transport paths become blocked for hydrocarbon transport and alternative (longer) paths have to be taken by the liquid. Hence, the reduction of permeability of water-rich liquids in γ -600 and γ -450 membranes can be understood in terms of a collective effect of porosity and tortuosity changes. The ratio ϵ/τ in eq 2 decreases in the presence of water, and therefore the permeability coefficient of water-containing liquids is smaller. This effect is most pronounced in the γ -450 membrane, which has the largest fraction of small pores. Because of the higher solubility of water in toluene, the critical pore size r_K for phase separation is larger in the water-hexane system. The fraction of pores that is blocked by water will therefore be smaller when toluene is used than when hexane is used. This could explain why the permeability differences between water-lean and water-rich hydrocarbons are larger in the γ -450 membrane than in the γ -600 membrane and why toluene is transported more easily than hexane. Since no substantial differences were observed between the permeabilities of water-lean and water-rich hydrocarbons in the γ -800 membrane, it seems that the pores in that membrane are wide enough to prevent spontaneous capillary condensation of water.

As was shown in Figure 4 and Table 4, water-rich hexane and toluene both need a certain threshold pressure to be

(17) Christenson, H. K.; Blom, C. E. *J. Chem. Phys.* **1987**, *86*, 419.

(18) Christenson, H. K. *J. Colloid Interface Sci.* **1985**, *104*, 234.

(19) Christenson, H. K.; Fang, J.; Israelachvili, J. N. *Phys. Rev. B* **1989**, *39*, 11750.

(20) Evans, R.; Marconi, U. M. B. *J. Chem. Phys.* **1987**, *86*, 7138.

(21) Fowkes, F. M. *Ind. Eng. Chem.* **1964**, *56*, 40.

(22) Riddick, J. A.; Toops, E. E., Jr. *Organic Solvents, Physical Properties and Methods of Purification*; Interscience Publishers: New York, 1955; Chapter III.

(23) Lippens, B. C.; Linsen, B. G.; De Boer, J. H. *J. Catal.* **1964**, *3*, 32.

(14) Christenson, H. K. *J. Phys. Chem.* **1986**, *90*, 4.

(15) Granick, S. *Science* **1991**, *253*, 1374.

(16) Christenson, H. K.; Horn, R. G.; Israelachvili, J. N. *J. Colloid Interface Sci.* **1982**, *88*, 79.

exceeded before liquid flow through the membrane commences. This phenomenon may be understood by considering the occurrence of two different types of flow under the experimental conditions, namely, spontaneous imbibition (displacement of a less wetting fluid by a more wetting fluid) and pressure-driven drainage (displacement of a more wetting fluid by a less wetting fluid).²⁴ These two competitive processes make the permeation process complicated to describe. The threshold pressure is most likely required to open up some of the water-blocked membrane pores by drainage working against the capillary pressure (or Laplace pressure) of the condensed water phase inside the largest blocked membrane pores.²⁵ Under completely water-free conditions, the flux versus pressure plot should follow Darcy's law once the pores have opened. However, since we are dealing with water-rich hydrocarbon feeds, spontaneous recondensation of water¹⁷ may occur as soon as a sufficiently large volume of water-rich hydrocarbon has entered and passed the membrane pores. This would ultimately lead to pore blocking again if no sufficient pressure is applied to keep these pores open.

The spreading coefficients of toluene and hexane on water should also be considered in this discussion. Although the alumina surface is a high-energy surface on which any type of liquid can spread spontaneously, it is reasonable to assume that at least a very thin layer of physisorbed water has formed on the inner and outer alumina surface, over which the hydrocarbon liquid has to pass to be transported. The equilibrium-spreading coefficient of toluene on water is zero, whereas the same coefficient for hexane is negative (-0.5).²⁶ A value of zero is a sufficient condition for spontaneous spreading, but a negative value suggests that only partial wetting will occur. It is therefore possible that full wetting of the membrane pores by hydrocarbons and net hydrocarbon transport will occur only when a certain minimum pressure is applied on the liquid.

Figure 6 illustrates how the liquid fluxes tend to decrease slowly with time for both water-lean and water-rich hexane. The decline of permeability of the water-rich liquid seems to occur slightly faster than with the water-lean liquid. The permeability decrease of both liquids may be attributed at least partly to ongoing capillary condensation of water from the hydrocarbon feeds that are constantly being supplied during the experiment. As the

amount of water that is supplied per unit time is small, the blocking of pores that are small enough for capillary condensation may continue for a considerable period of time during which the permeability decreases gradually. This explanation may also hold for the water-lean system as it also does contain some water (<0.001 mol/l).

Alternatively, it is also possible that the gradual flux decrease is somehow related to phenomena occurring in the hydrocarbon phase. It has been reported⁸ that solvent molecules may become strongly adsorbed and immobilized on γ -alumina surfaces during organic liquid transport. Such an adsorption process would lead to a gradual reduction of the effective pore size available for transport and thereby to a reduction of solvent permeability. In the case that traces of water are also present, phase separation of water and adsorption of organic molecules may work synergistically in reducing the permeability with time.

5. Conclusions

We have shown that the permeability of liquids is affected by the membrane pore size and the water content of organic liquids. A very low molar fraction ($\sim 5 \cdot 10^{-4}$) of dissolved water in hydrophobic solvents was shown to decrease the permeability of toluene and hexane through γ -alumina membranes with pore diameters <6 nm considerably. This effect was explained by the occurrence of phase separation and capillary condensation of water from the hydrocarbon phase, which leads to pore blocking of small pores. The presence of water as a trace component was also shown to lead to phenomena like a nonzero cutoff pressure for liquid flow, which was not observed with water-lean solvents. Water-lean hexane and toluene had similar permeability coefficients for a given membrane, but different permeabilities were observed when water was present. In the latter cases, the less polar solvent hexane exhibited a lower permeability than toluene. This is probably related to the higher relative activity of water in hexane than in toluene, which leads to blocking of larger pores, and possibly to more physisorption of water on nonblocked pore walls.

Acknowledgment. Financial support of the Commission of the EC in the framework of the Growth Program contract no. G1RD-2000-00347 (SUSTOX) is gratefully acknowledged. S.R.C. thanks Dr. H. K. Christenson, The University of Leeds, U.K. for constructive discussions and encouragement.

LA0364237

(24) Hashemi, M.; Dabir, B.; Sahimi, M. *AIChE J.* **1999**, *45*, 1365.

(25) Schneider, P.; Uchytil, P. *Membr. Sci.* **1994**, *95*, 29.

(26) Dobbs, H.; Bonn, D. *Langmuir* **2001**, *17*, 4674.